The G4 Resolvase Dhx36 Modulates Cardiomyocyte Differentiation and Ventricular Conduction System Development

Authors: Pablo Gómez-del Arco[1,2] *, Joan Isern[3,4], Daniel Jimenez-Carretero[5], Dolores López-Maderuelo[2,€], Rebeca Piñeiro-Sabarís[6, 7], Fadoua El Abdellaoui-Soussi[1,2,£], Carlos Torroja[5], María Linarejos Vera-Pedrosa[8], Mercedes Grima-Terrén[3,4], Alberto Benguria[9], Ana Simón-Chica[10], Antonio Queiro-Palou[1,2,#], Ana Dopazo[9], Fátima Sánchez-Cabo[5], José Jalife [8,11], José Luis de la Pompa[6,7], David Filgueiras-Rama[7,10,12], Pura Muñoz-Cánoves[3,4,13,14] * and Juan Miguel Redondo[2,7,15] *

Affiliations: 1, Institute for Rare Diseases Research, Instituto de Salud Carlos III (ISCIII). Majadahonda, Madrid, Spain. 2, Gene Regulation in Cardiovascular Remodelling and Inflammation Laboratory, Centro Nacional de Investigaciones Cardiovasculares Carlos III (CNIC). Madrid, Spain. 3, Altos Labs, Inc., San Diego Institute of Science, San Diego, CA, USA. 4, Tissue Regeneration Laboratory, Centro Nacional de Investigaciones Cardiovasculares Carlos III (CNIC). Madrid, Spain. 5, Bioinformatics Unit, Centro Nacional de Investigaciones Cardiovasculares Carlos III (CNIC). Madrid, Spain. 6, Intercellular Signaling in Cardiovascular Development and Disease Laboratory, Centro Nacional de Investigaciones Cardiovasculares Carlos III (CNIC). Madrid, Spain. 7, Centro de Investigación Biomédica en Red de Enfermedades Cardiovasculares (CIBERCV). Madrid, Spain. 8, Cardiac Arrhythmia Laboratory, Centro Nacional de Investigaciones Cardiovasculares Carlos III (CNIC). Madrid, Spain. 9, Genomics Unit, Centro Nacional de Investigaciones Cardiovasculares Carlos III (CNIC). Madrid, Spain. 10, Novel Arrhythmogenic Mechanisms Program, Centro Nacional de Investigaciones Cardiovasculares Carlos III (CNIC). Madrid, Spain. 11, University of Michigan, Ann Arbor, MI, USA. 12, Cardiovascular Institute, Instituto de Investigación Sanitaria del Hospital Clínico San Carlos (IdISSC). Madrid, Spain. 13, Department of Experimental & Health Sciences, University Pompeu Fabra (UPF)/CIBERNED. Barcelona, Spain. 14, Catalan Institution for Research and

Advanced Studies (ICREA), Barcelona, Spain. 15, Cell-Cell Communication & Inflammation Unit, Centro de Biología Molecular Severo Ochoa (CBMSO), Consejo Superior de Investigaciones Científicas-Universidad Autónoma de Madrid. Madrid, Spain. €, present address, Microscopy and Dynamic Imaging Unit, Centro Nacional de Investigaciones Cardiovasculares Carlos III (CNIC). Madrid, Spain. £, present address, Center for Stem Cells and Organoid Medicine (CuSTOM), Cincinnati Children's Hospital Medical Center, Cincinnati, OH, USA. #, present address, department of Medical Biochemistry and Biophysics, Karolinska Institute, Stockholm, Sweden.

Supplementary information

Table of contents

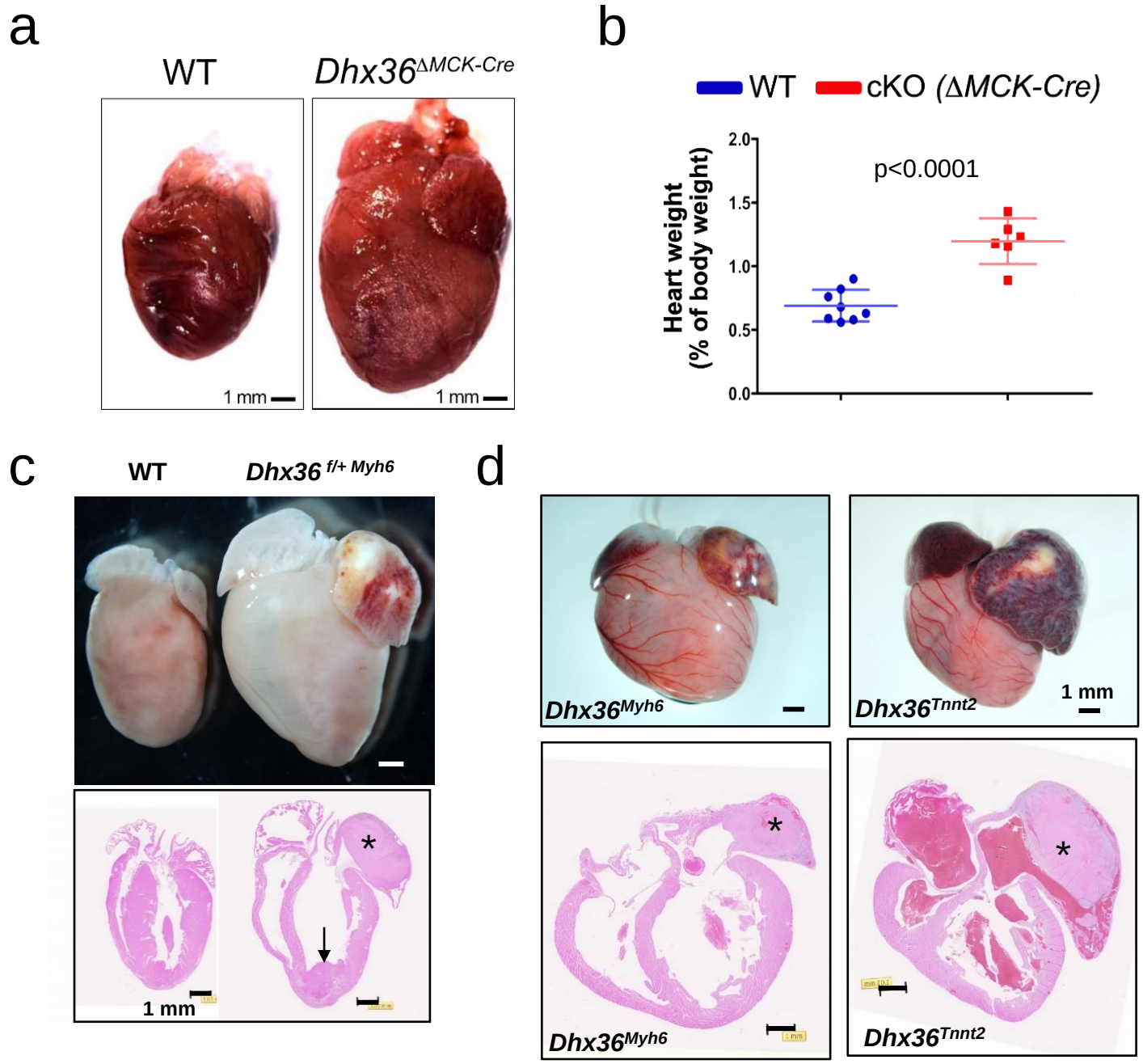

Supplementary Fig. 1. Cardiac deletion of *Dhx36* induces dilated cardiomyopathy and atrial thrombosis in adult mice. a, Gross morphology of hearts from WT and *Dhx36*$^{f/f}$;*MCK*$^{Cre/wt}$ (*Dhx36*$^{\Delta MCK\text{-}Cre}$) mice. **b,** Heart weight-to-body weight ratios of WT (n=8) and *Dhx36* $^{\Delta MCK\text{-}Cre}$ (n=6) mice. Statistical significance was assessed using an unpaired two-sided t-test, with data presented as mean ± SEM. **c**, Gross cardiac morphology and hematoxylin & eosin (H&E) staining on heart sections from a WT mouse and a sick 284-day-old heterozygous *Dhx36*^{Myh6} (*Dhx36*$^{f/+\ Myh6}$) littermate. Thrombi in the left atrium (asterisk) and left ventricle (arrow) of the mutant are indicated. **d**, Gross cardiac morphology and H&E staining of hearts sections from autopsied *Dhx36*^{Myh6} and *Dhx36*^{Tnnt2} mice, both showing thrombi occupying the entire left atrium (asterisks). All scale bars represent 1 mm.

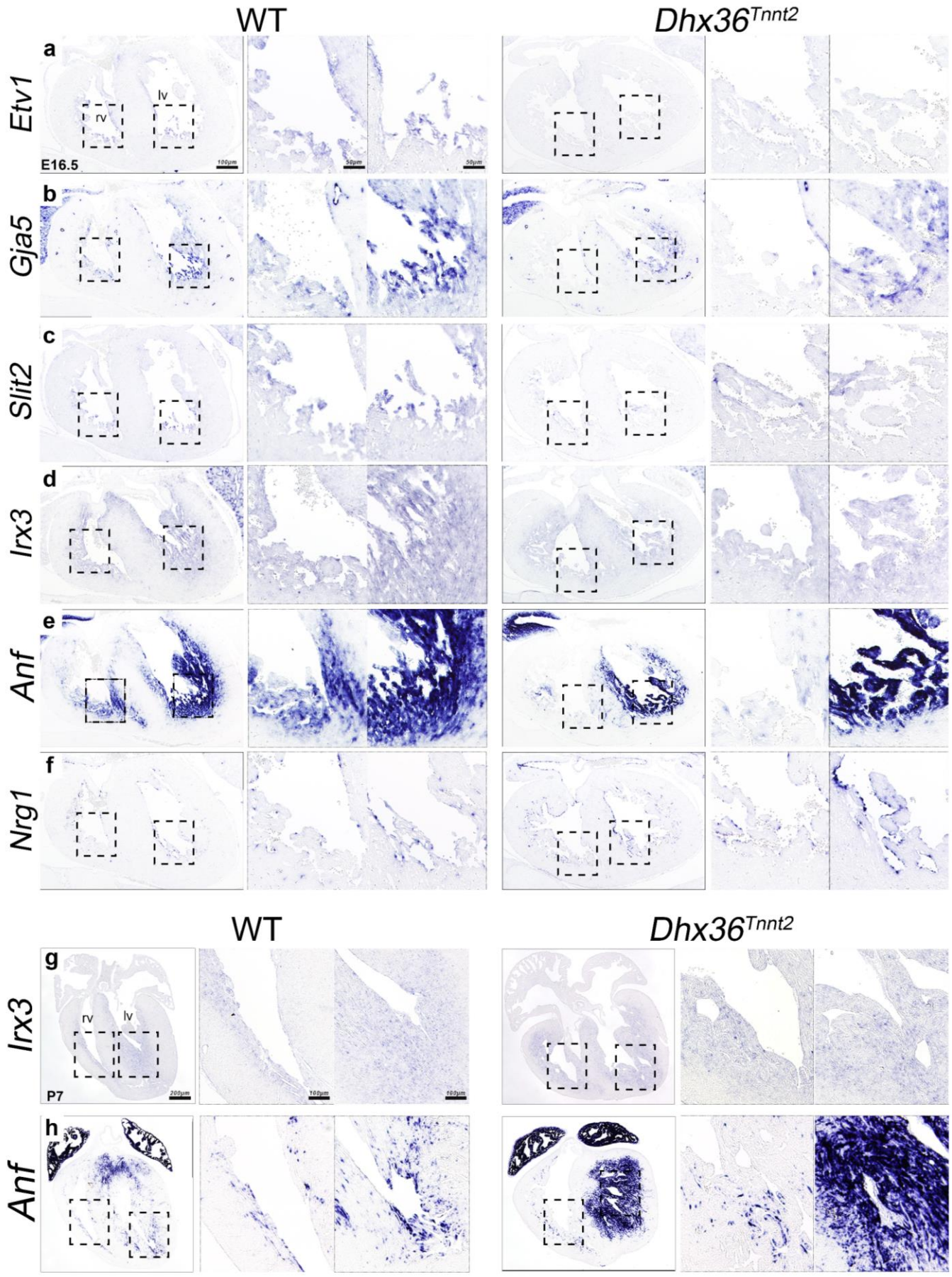

Supplementary Fig. 2. Disruption of critical conduction system markers in *Dhx36^{Tnnt2}* mutant hearts. In situ hybridization (ISH) analysis of various conduction system markers in ED16.5 (**a-f**) and PD7 (**g,h**) hearts, showing representative images from wild type (WT) and *Dhx36^{Tnnt2}* mutant hearts. Abbreviations: lv, left ventricle, rv, right ventricle. Scale bars, 100 µm in a-f (general heart views), 50 µm in a-f (high magnification views); 200 µm in g,h (general heart views), 100 µm in g,h (high magnification views). The scale bars are shown in the first ISH image of WT hearts for reference and apply to all corresponding images, as they present the same magnifications.

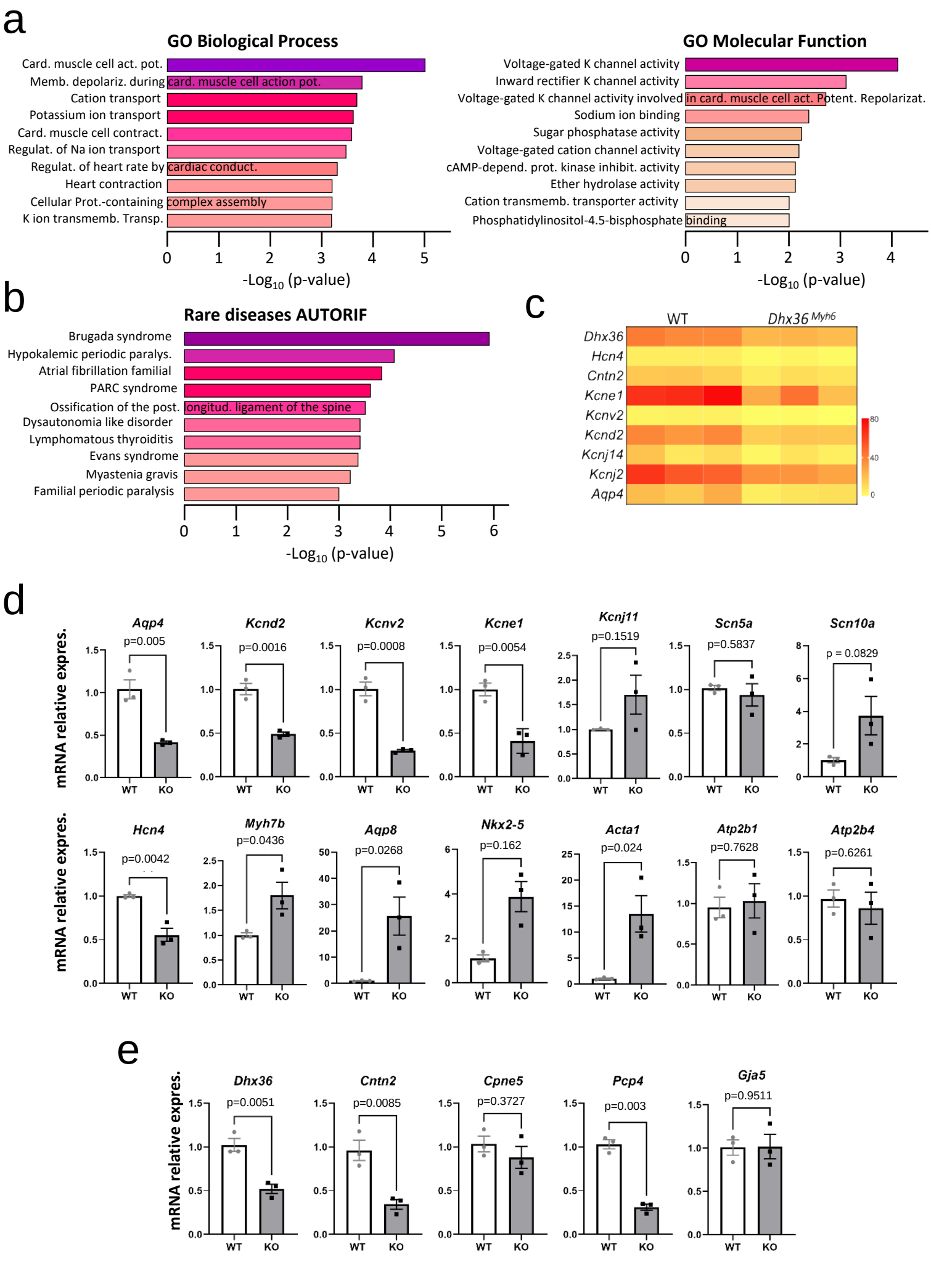
a
GO Biological Process
Card. muscle cell act. pot.
Memb. depolariz. during
Cation transport
Potassium ion transport
Card. muscle cell contract.
Regulat. of Na ion transport
Regulat. of heart rate by
Heart contraction
Cellular Prot.-containing
K ion transmemb. Transp.
card. muscle cell action pot.
cardiac conduct.
complex assembly
0 1 2 3 4 5
-Log10 (p-value)
GO Molecular Function
Voltage-gated K channel activity
Inward rectifier K channel activity
Voltage-gated K channel activity involved
Sodium ion binding
Sugar phosphatase activity
Voltage-gated cation channel activity
cAMP-depend. prot. kinase inhibit. activity
Ether hydrolase activity
Cation transmemb. transporter activity
Phosphatidylinositol-4.5-bisphosphate
in card. muscle cell act. Potent. Repolarizat.
binding
0 1 2 3 4
-Log10 (p-value)
b
Rare diseases AUTORIF
Brugada syndrome
Hypokalemic periodic paralys.
Atrial fibrillation familial
PARC syndrome
Ossification of the post.
Dysautonomia like disorder
Lymphomatous thyroiditis
Evans syndrome
Myastenia gravis
Familial periodic paralysis
longitud. ligament of the spine
0 1 2 3 4 5 6
-Log10 (p-value)
c
WT
Dhx36 Myh6
Dhx36
Hcn4
Cntn2
Kcne1
Kcnv2
Kcnd2
Kcnj14
Kcnj2
Aqp4
80
40
0
d
mRNA relative expres.
Aqp4
p=0.005
Kcnd2
p=0.0016
Kcnv2
p=0.0008
Kcne1
p=0.0054
Kcnj11
p=0.1519
Scn5a
p=0.5837
Scn10a
p = 0.0829
Hcn4
p=0.0042
Myh7b
p=0.0436
Aqp8
p=0.0268
Nkx2-5
p=0.162
Acta1
p=0.024
Atp2b1
p=0.7628
Atp2b4
p=0.6261
WT
KO
e
mRNA relative expres.
Dhx36
p=0.0051
Cntn2
p=0.0085
Cpne5
p=0.3727
Pcp4
p=0.003
Gja5
p=0.9511
WT
KO

Supplementary Fig. 3. Dhx36 regulates the transcription of the cardiac conduction system gene program. **a**, Gene ontology (GO) analysis of biological processes and molecular functions associated with downregulated genes in 2–3-week-old *Dhx36*^{Myh6} mice compared to WT. **b,** Analysis of rare diseases associated with the downregulated genes identified in *Dhx36*^{Myh6} mice. **c**, Heat map illustrating the expression levels of selected cardiac conduction system genes from RNA-seq data. **d,** Quantitative PCR analysis of selected deregulated genes identified in RNA-seq data from cardiac tissue of 2–3-week-old *Dhx36*^{Myh6} (KO) mice, with WT expression levels normalized to 1. **e**, Quantitative PCR showing the expression of Dhx36 and additional selected cardiac conduction system genes in the same RNA samples. Statistical significance was determined using unpaired two-sided t-tests, with data presented as mean **±** SEM for panels **d** and **e**. Source data for **d** and **e** are provided in the accompanying source data file.

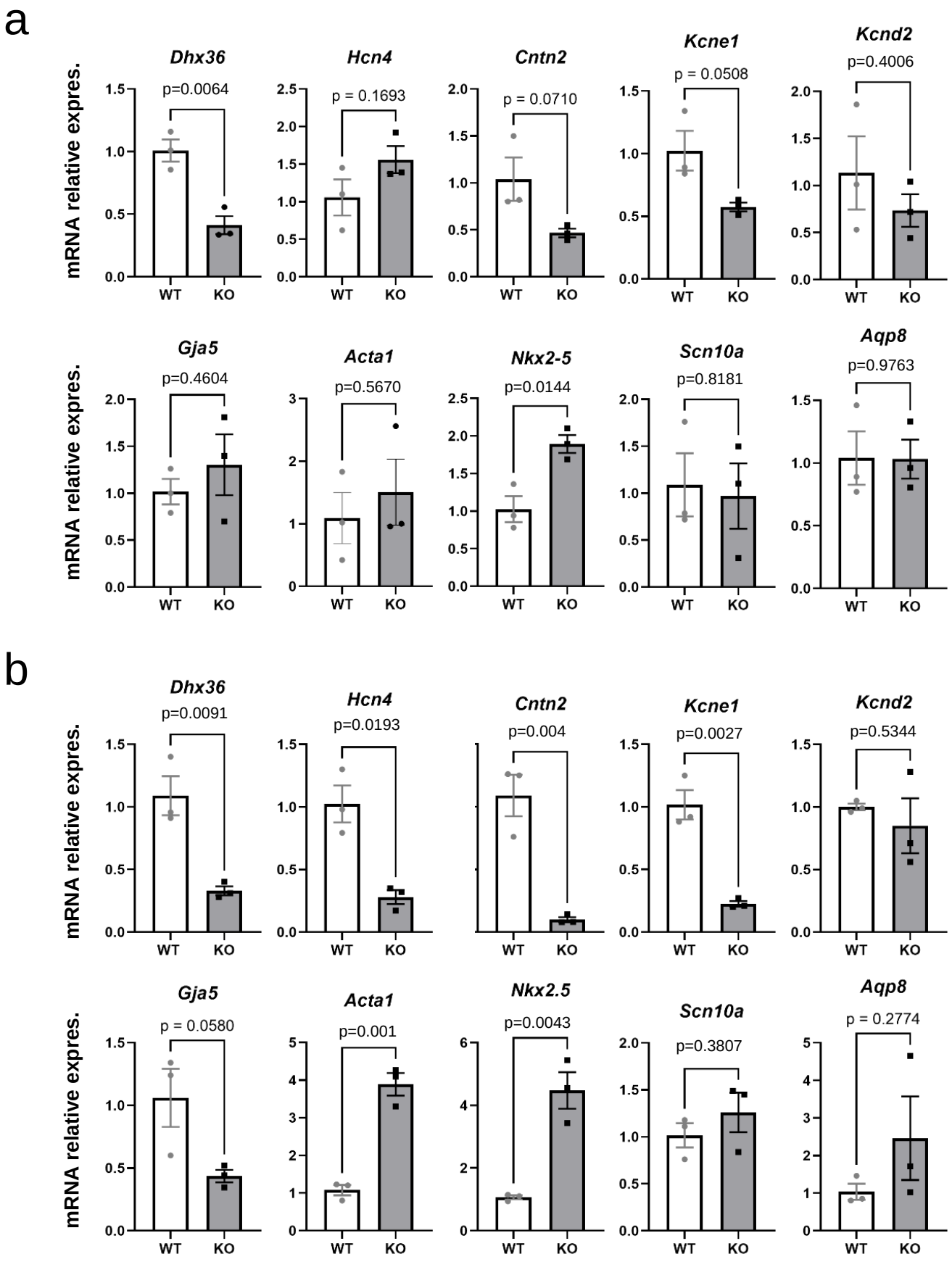

Supplementary Fig. 4. Quantitative PCR analysis of cardiac gene expression in neonatal *Dhx36*^{Myh6} and *Dhx36*^{TnnT2} mice. a, Quantitative PCR analysis of selected genes in cardiac muscle from PD0-PD1 *Dhx36*^{Myh6} (KO) neonates, compared to WT littermates. Data represent three pools of 3 neonates per pool (n=9 per genotype). **b**, Quantitative PCR analysis of selected genes in cardiac muscle from PD0-PD1 *Dhx36*^{Tnnt2} neonates (KO) compared to WT littermates, with the same sample pooling as in **a**. Statistical significance was determined using an unpaired two-sided t-test, with data presented as mean ± SEM. Source data are provided in the accompanying source data file.

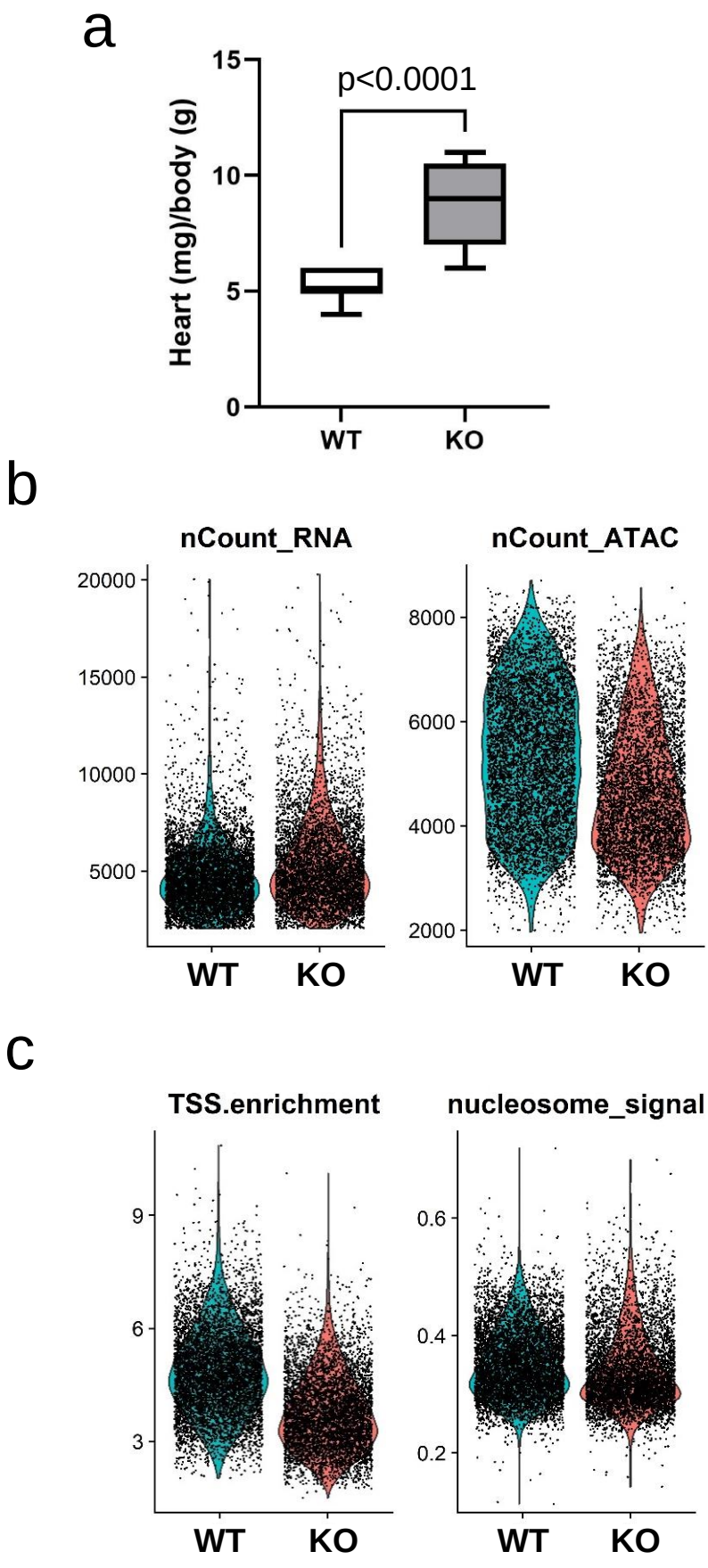

Supplementary Fig. 5. Quality controls metrics for multiome snATAC-seq and snRNA-seq analyses. a, Heart-to-body weight ratios of PD7 pups, indicating cardiac hypertrophy in mutant mice (KO) compared to WT. Statistical significance was determined using unpaired two-sided t-test, with data presented as mean ± SEM. Source data are provided in the accompanying source data file. **b**, Distribution of RNA counts per cell and DNA counts per cell sequenced in the snRNA-seq and ATAC-seq experiments, respectively, for WT and KO hearts. **c**, Transcription start site (TSS) enrichment scores comparing KO and WT, showing a reduction in TSS enrichment in the KO samples. Additionally, the nucleosome banding pattern (right) is presented for both genotypes.

a

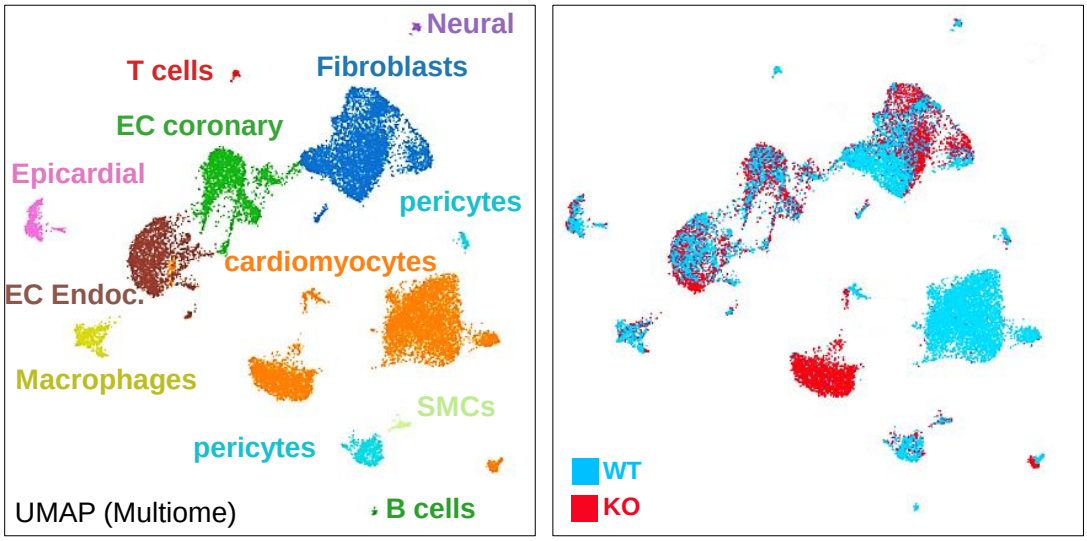
Neural
T cells
Fibroblasts
EC coronary
Epicardial
pericytes
cardiomyocytes
EC Endoc.
Macrophages
SMCs
pericytes
B cells
UMAP (Multiome)
WT
KO

b

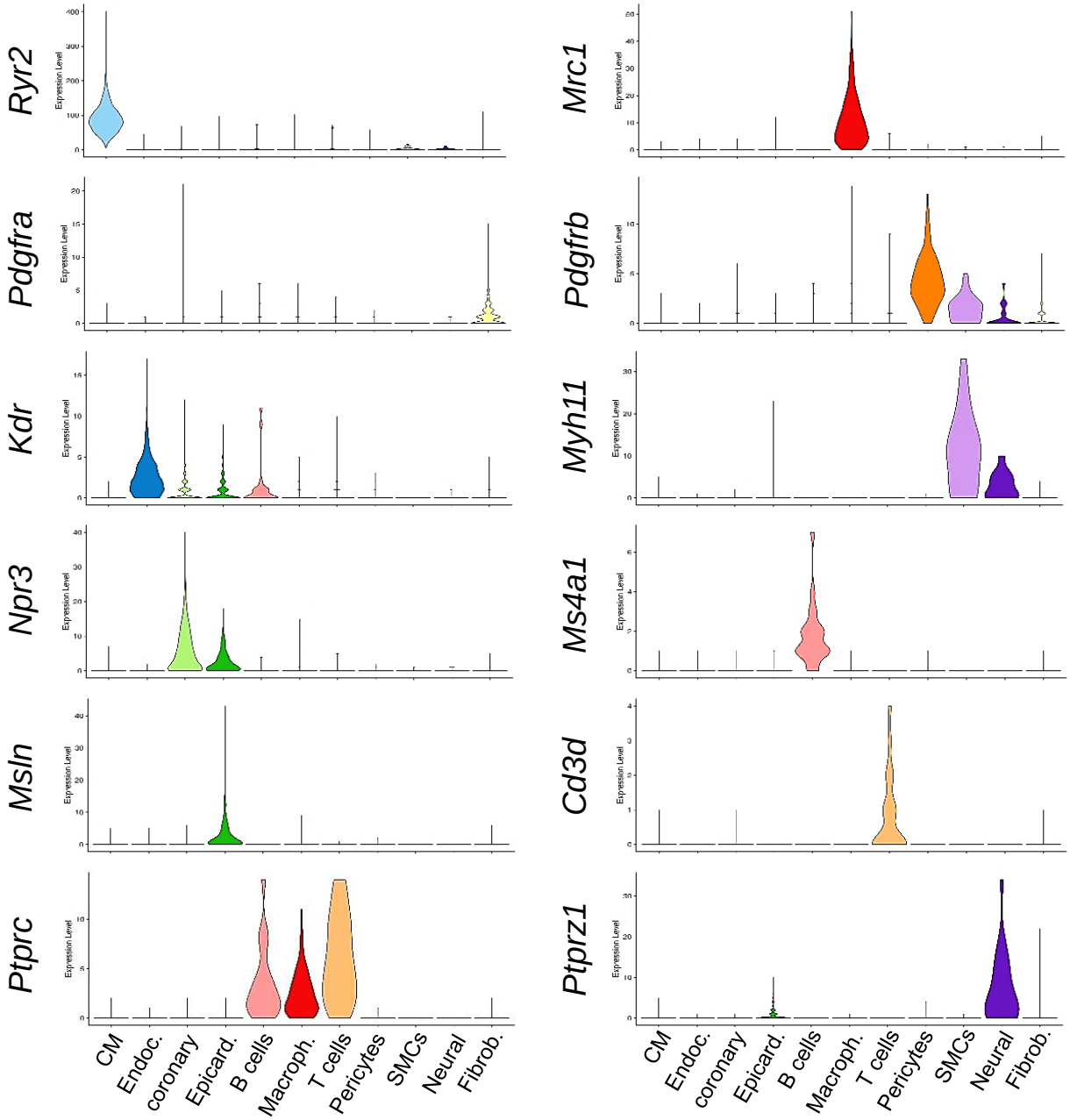
Ryr2
Mrc1
Pdgfra
Pdgfrb
Kdr
Myh11
Npr3
Ms4a1
Msln
Cd3d
Ptprc
Ptprz1
Expression Level
CM
Endoc.
coronary
Epicard.
B cells
Macroph.
T cells
Pericytes
SMCs
Neural
Fibrob.

Supplementary Fig. 6. Integrated multiome snATAC-seq and snRNA-seq analysis of nuclei clusters in WT and mutant PD7 hearts. a, Multimodal Uniform Manifold Approximation and Projection (UMAP) visualization of cell clusters from WT and KO PD7 hearts. The left panel shows cell clusters randomly colored by cluster identity (WT; n=6,499; KO, n=5,426). The right panel displays the same UMAP, colored by sample origin (WT in blue, KO in red). **b**, Violin plots depicting the expression levels of representative genes across different cell clusters, illustrating the transcriptional profiles in WT hearts. Cell clusters names defined in the MS text and in Legend of Fig. 5.

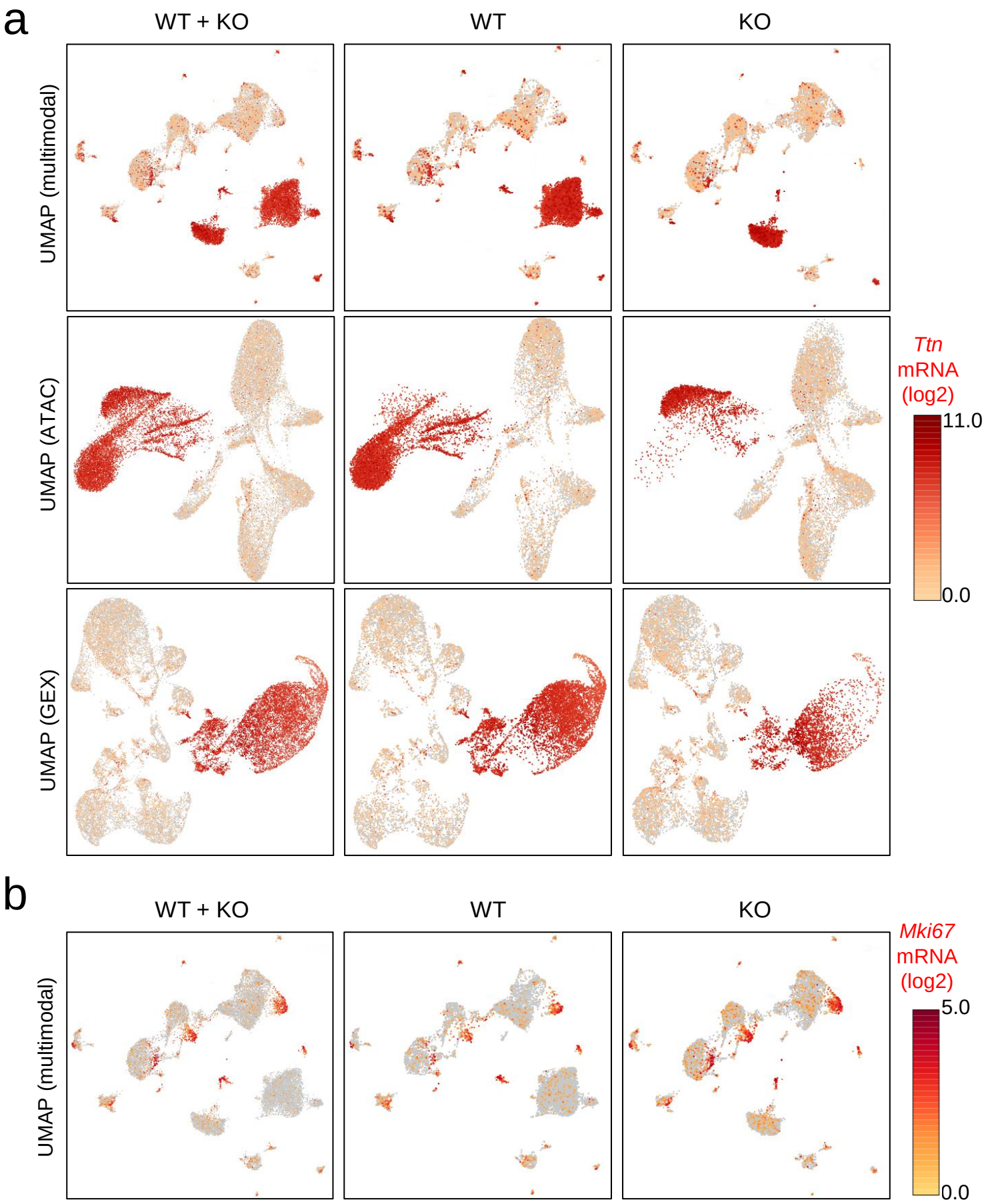

Supplementary Fig. 7. Comparison of Multiome snATAC-seq and RNA-seq with unimodal UMAPs and proliferation signatures. a, Multiome UMAP visualization integrating snATAC-seq and snRNA-seq data from both WT and KO hearts (upper left). Separate UMAPs display *Titin* (*Ttn*) expression in WT (upper middle) and KO (upper right) hearts. The middle panel shows UMAP plots based on ATAC-seq data, while the lower panel presents UMAP plots based on RNA-seq data (Gene Expression [GEX]). **b,** Multiome UMAPs as in (**a**), displaying the expression of the proliferative gene Mki67 in WT and KO hearts.

a

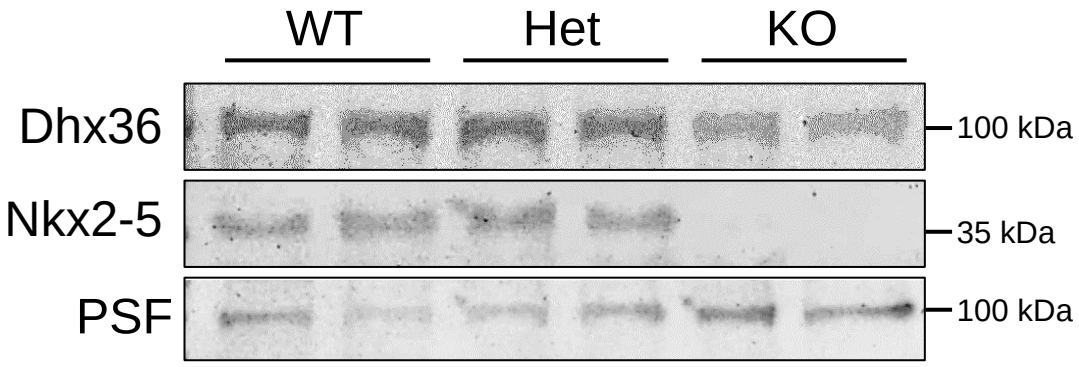

b

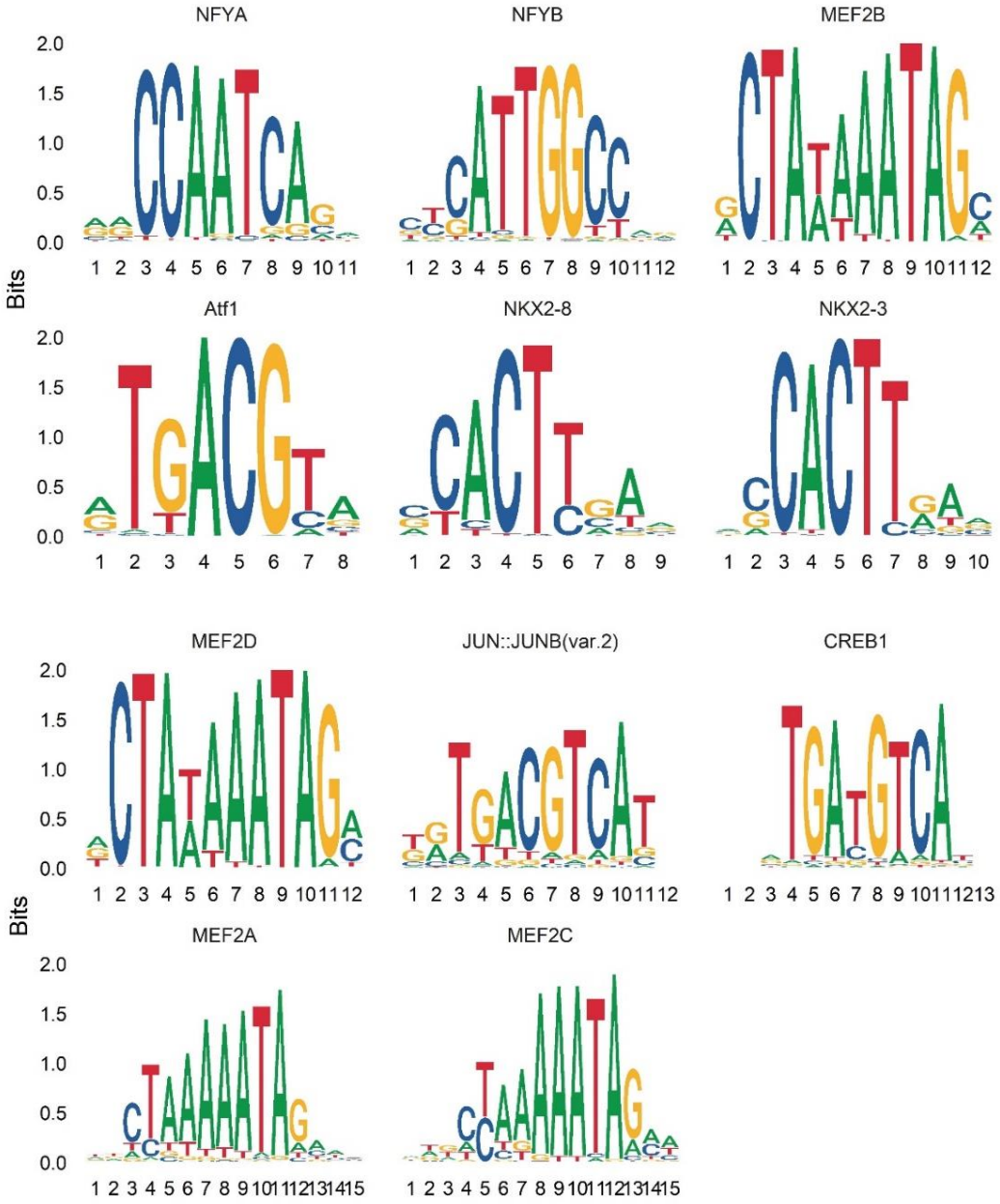

Supplementary Fig. 8. Protein expression and motif enrichment analysis in gene promoters of CMs in PD7 hearts. a, Western blotting analysis showing reduced expression of Dhx36 and complete absence of Nkx2-5 in mutant PD7 hearts (KO; n=2), compared to heterozygous (Het; n=2) or WT (n=2). PSF (PTB-associated splicing factor) was used as a loading control in the same blot where Nkx2-5 was detected. **b**, Position weight matrices plots representing the motifs of transcription factors that are downregulated in KO cardiomyocytes compared to WT. Uncropped images for Supplementary Fig. 8a are provided at the end of this Supplementary file.

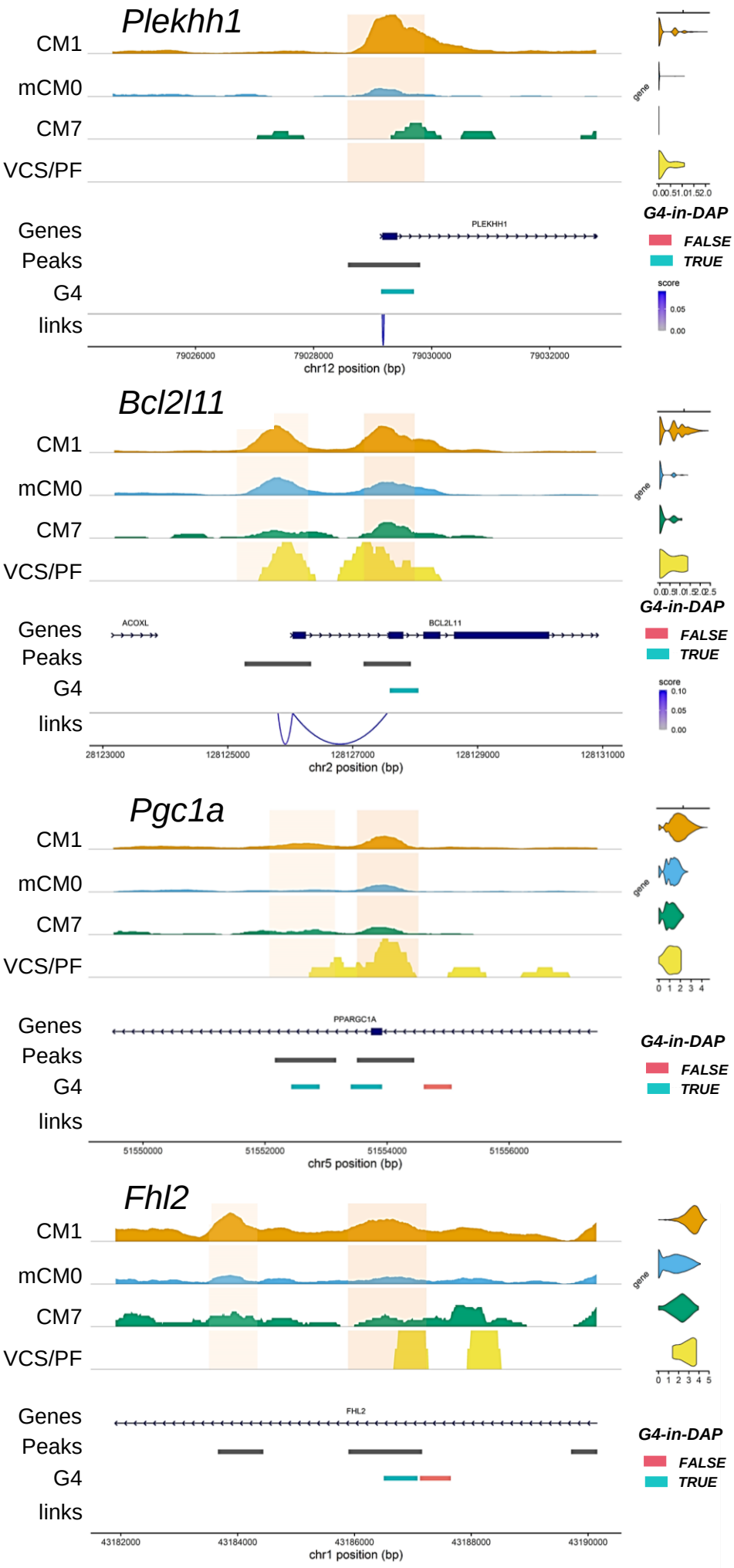
Plekhh1
CM1
mCM0
CM7
VCS/PF
Genes
Peaks
G4
links
PLEKHH1
79026000
79028000
79030000
79032000
chr12 position (bp)
gene
G4-in-DAP
FALSE
TRUE
score
0.05
0.00
Bcl2l11
ACOXL
BCL2L11
28123000
128125000
128127000
128129000
128131000
chr2 position (bp)
0.10
Pgc1a
PPARGC1A
51550000
51552000
51554000
51556000
chr5 position (bp)
Fhl2
FHL2
43182000
43184000
43186000
43188000
43190000
chr1 position (bp)

Supplementary Fig. 9. G-quadruplex (G4) structures and transcriptional alterations in downregulated Dhx36 gene targets. Examples of downregulated genes (*Plekhh1*, *Bcl2l11*, *Ppargc1a* (*Pgc1a*) and *Fhl2*) in KO CMs that contain G4 motifs overlapping with regions of open chromatin in their promoters (TRUE). For a detailed explanation, refer to the legend of Fig. 8.

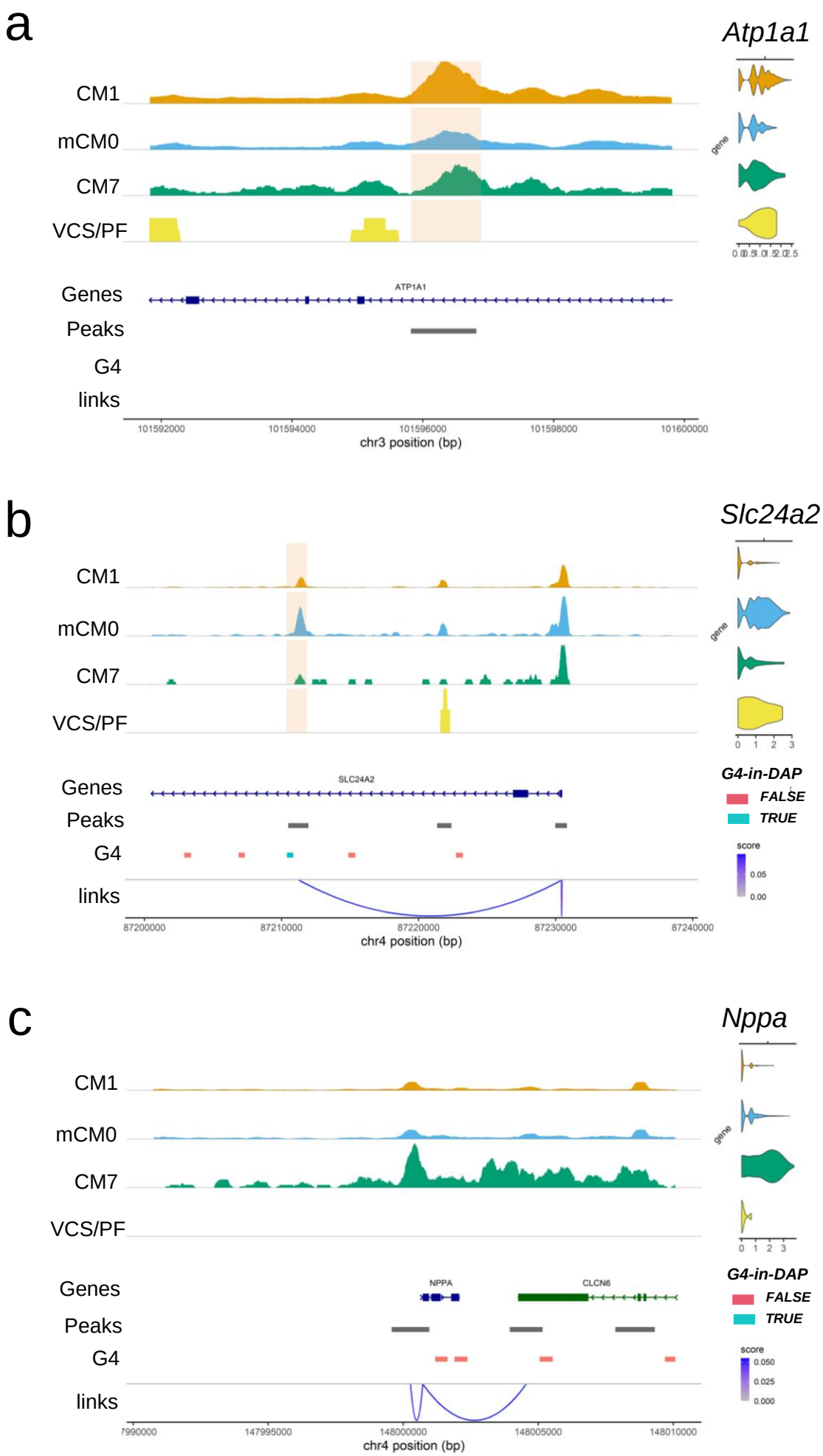
a
Atp1a1
CM1
mCM0
CM7
VCS/PF
gene
Genes
Peaks
G4
links
ATP1A1
101592000
101594000
101596000
101598000
101600000
chr3 position (bp)
b
Slc24a2
CM1
mCM0
CM7
VCS/PF
gene
Genes
Peaks
G4
links
SLC24A2
G4-in-DAP
FALSE
TRUE
score
0.05
0.00
87200000
87210000
87220000
87230000
87240000
chr4 position (bp)
c
Nppa
CM1
mCM0
CM7
VCS/PF
gene
Genes
Peaks
G4
links
NPPA
CLCN6
G4-in-DAP
FALSE
TRUE
score
0.050
0.025
0.000
7990000
147995000
148000000
148005000
148010000
chr4 position (bp)

Supplementary Fig. 10. G4 structures and transcriptional alterations of representative Dhx36 gene targets. a, Example of a downregulated gene (*Atp1a1*) in KO CMs that do not contain G4s motifs overlapping with open chromatin in its promoter. **b**, Example of an upregulated gene (*Slc24a2*) in KO CMs that contains G4s motifs overlapping with open chromatin in its promoter (TRUE). C. Example of stress gene *Anf* (*Nppa*), which is upregulated in KO CMs and does not contain G4s motifs overlapping with open chromatin in its promoter. For a detailed explanation, refer to the legend of Fig. 8.

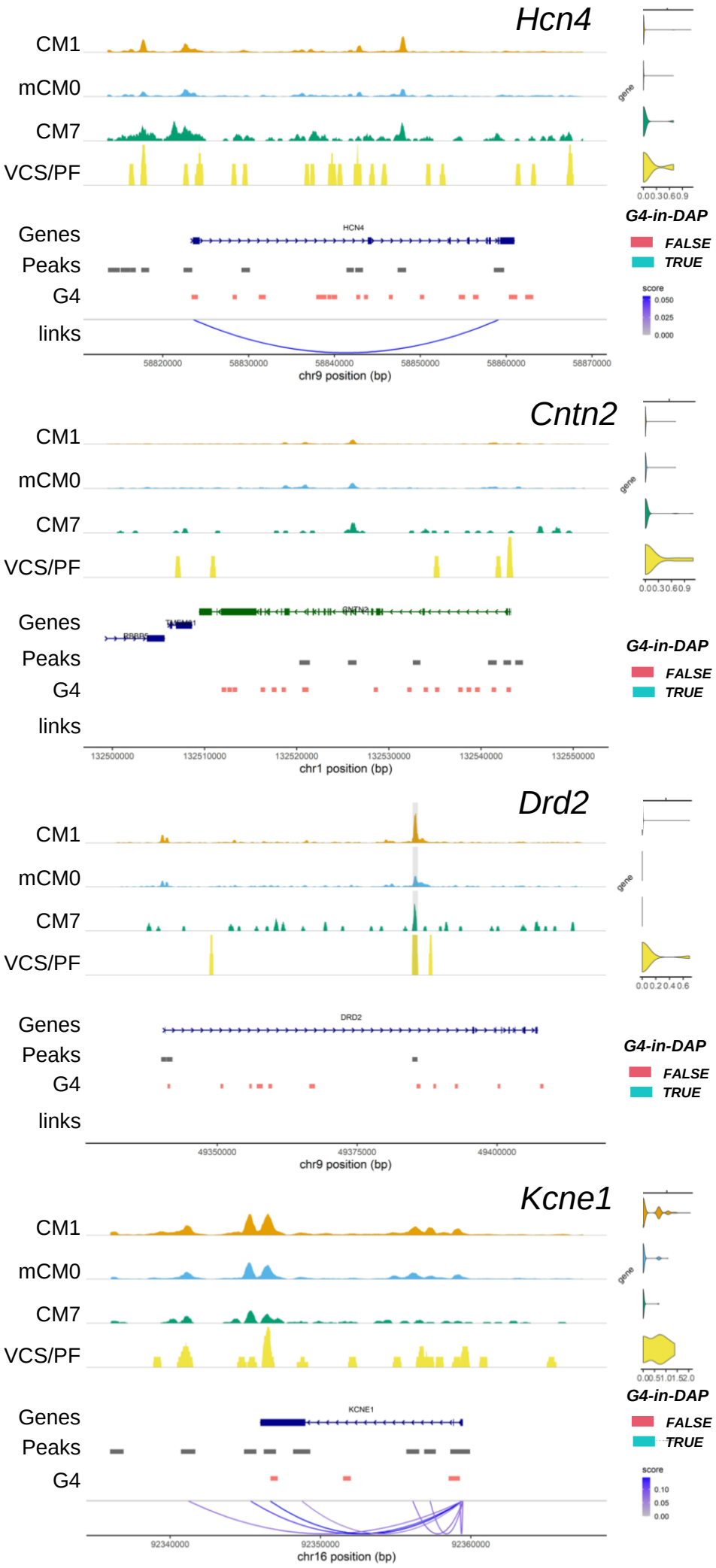
Hcn4
CM1
mCM0
CM7
VCS/PF
Genes
Peaks
G4
links
HCN4
58820000
58830000
58840000
58850000
58860000
58870000
chr9 position (bp)
gene
0.0 0.3 0.6 0.9
G4-in-DAP
FALSE
TRUE
score
0.050
0.025
0.000
Cntn2
CM1
mCM0
CM7
VCS/PF
Genes
Peaks
G4
links
CNTN2
132500000
132510000
132520000
132530000
132540000
132550000
chr1 position (bp)
gene
0.0 0.3 0.6 0.9
G4-in-DAP
FALSE
TRUE
Drd2
CM1
mCM0
CM7
VCS/PF
Genes
Peaks
G4
links
DRD2
49350000
49375000
49400000
chr9 position (bp)
gene
0.0 0.2 0.4 0.6
G4-in-DAP
FALSE
TRUE
Kcne1
CM1
mCM0
CM7
VCS/PF
Genes
Peaks
G4
KCNE1
92340000
92350000
92360000
chr16 position (bp)
gene
0.0 0.5 1.0 1.5 2.0
G4-in-DAP
FALSE
TRUE
score
0.10
0.05
0.00

Supplementary Fig. 11. G4 structures and transcriptional alterations in Dhx36 gene targets within the cardiac conduction system. This figure illustrates a subset of genes involved in the cardiac conduction system (CCS) that exhibit downregulation in knockout (KO) cardiomyocytes (CMs). These genes are characterized by the presence of G4 structures within their gene bodies.

Luciferase Activity: Relative Light Units (R.L.U)

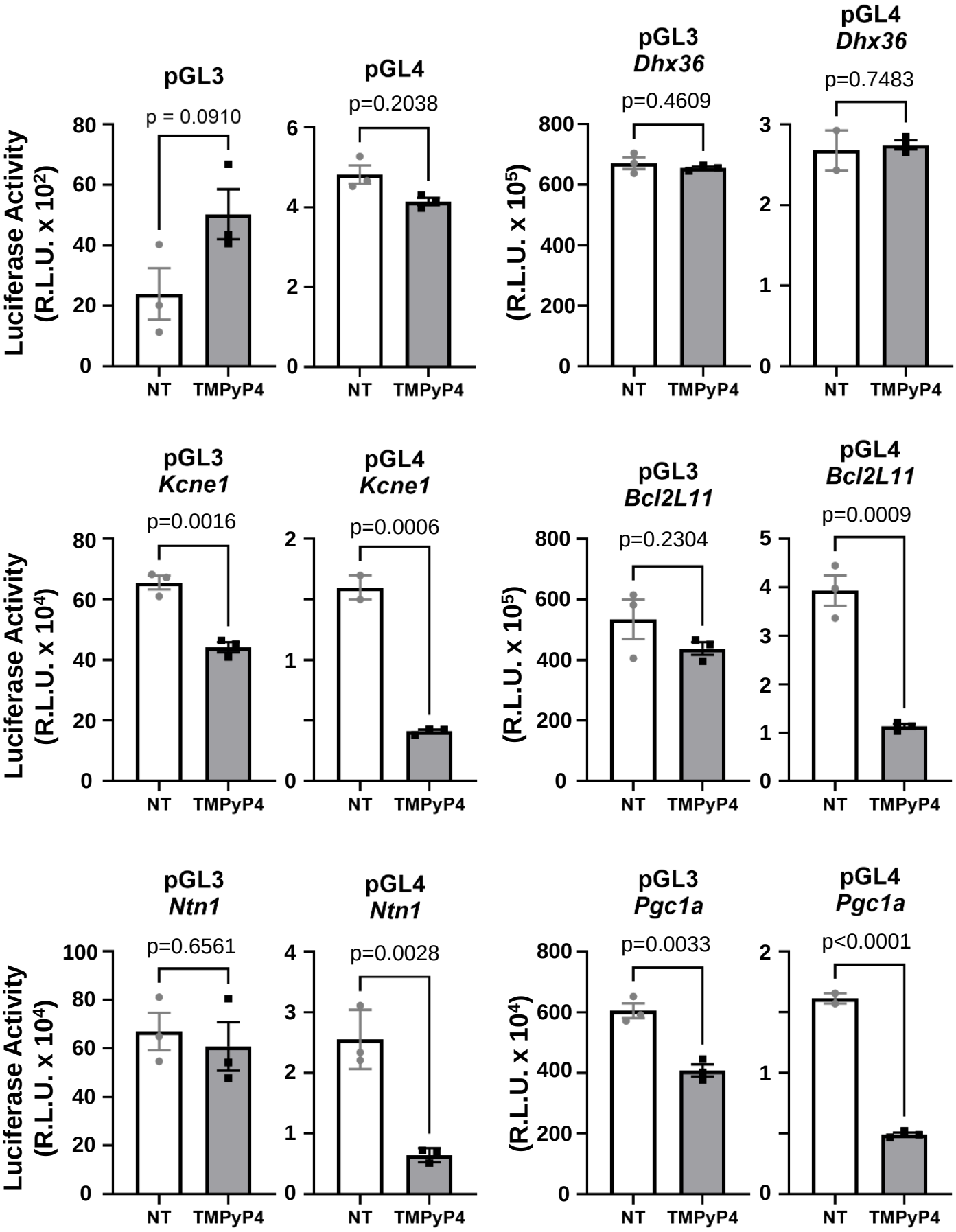

Supplementary Fig. 12. G4 structures regulate the transcription of Dhx36 gene targets in cardiomyocytes. Luciferase reporter assays conducted in HeLa cells to investigate the transcriptional activity of promoter regions from putative Dhx36 target genes, as identified in Fig. 9. The activities of both pGL3 and pGL4.25 promoter constructs are shown under conditions of G4 stabilization by the drug TMPyP4 (20 μM) and without treatment (NT; not treated). The results indicate that G4-resolvase activity is essential for transcriptional activation in these promoters. As a control, the *Dhx36* promoter, which lacks G4 structures, is included to demonstrate transcriptional activity independent of G4 resolution. Empty pGL3-basic and pGL4.25 (pGL4) plasmids serve as negative controls. Statistical significance was determined using unpaired two-sided t-tests, with data presented as mean ± SEM.

Uncropped blots Supplementary Figure 8a

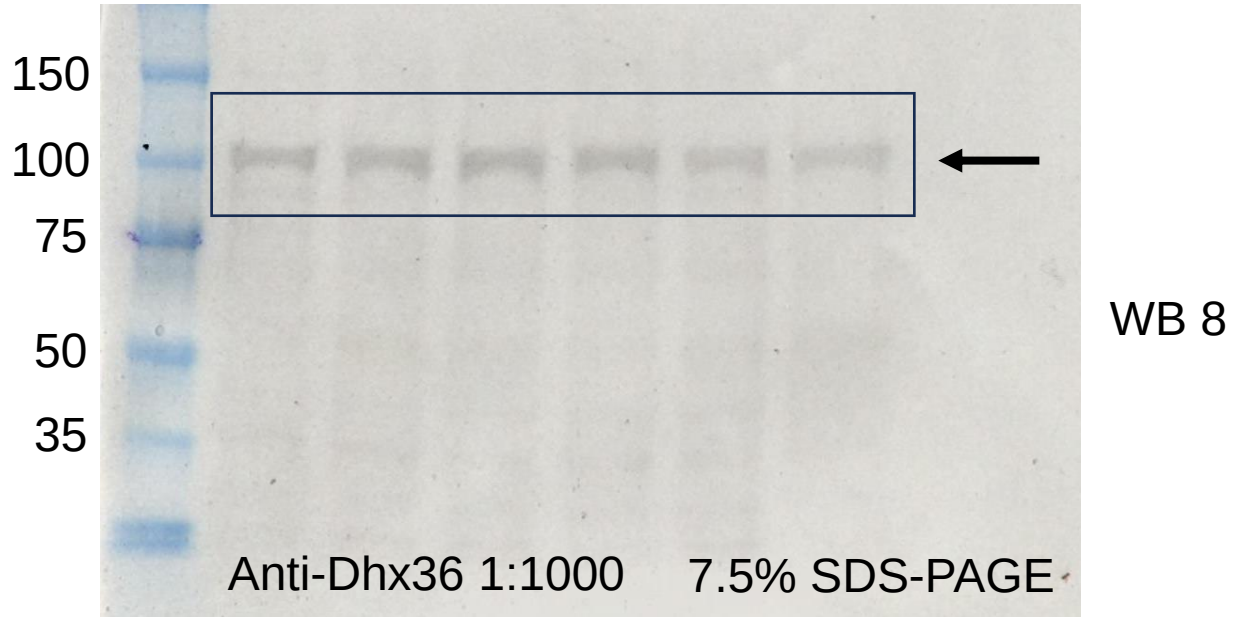

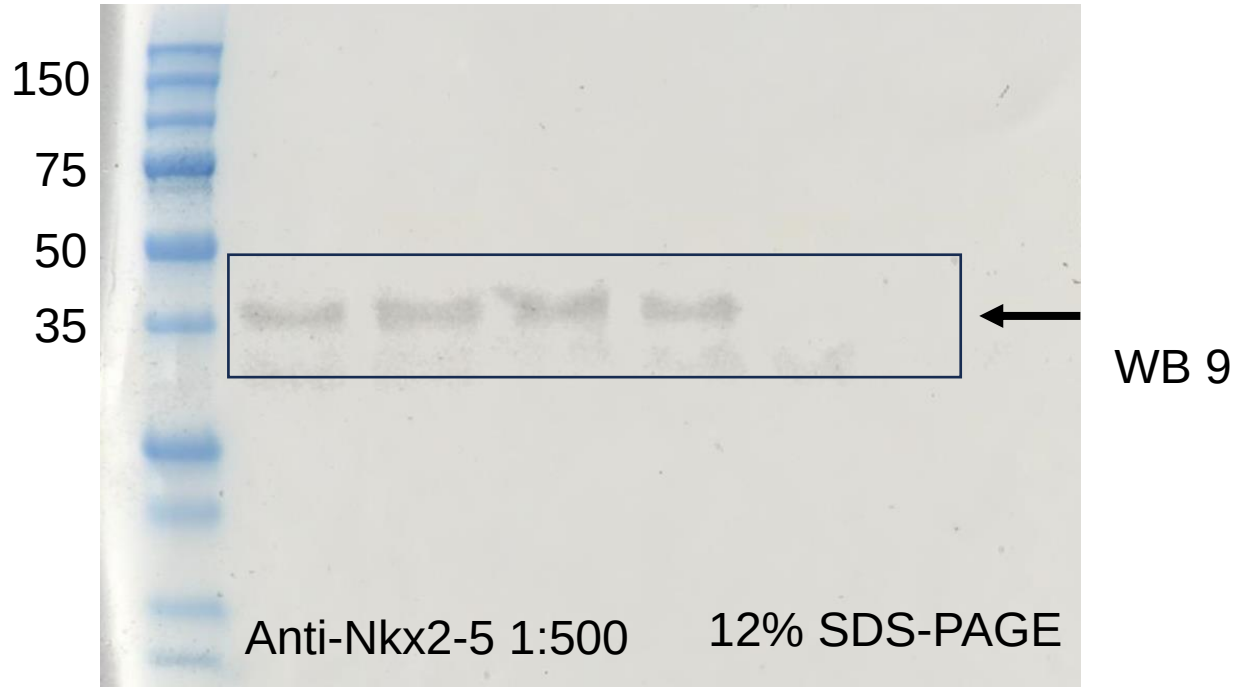

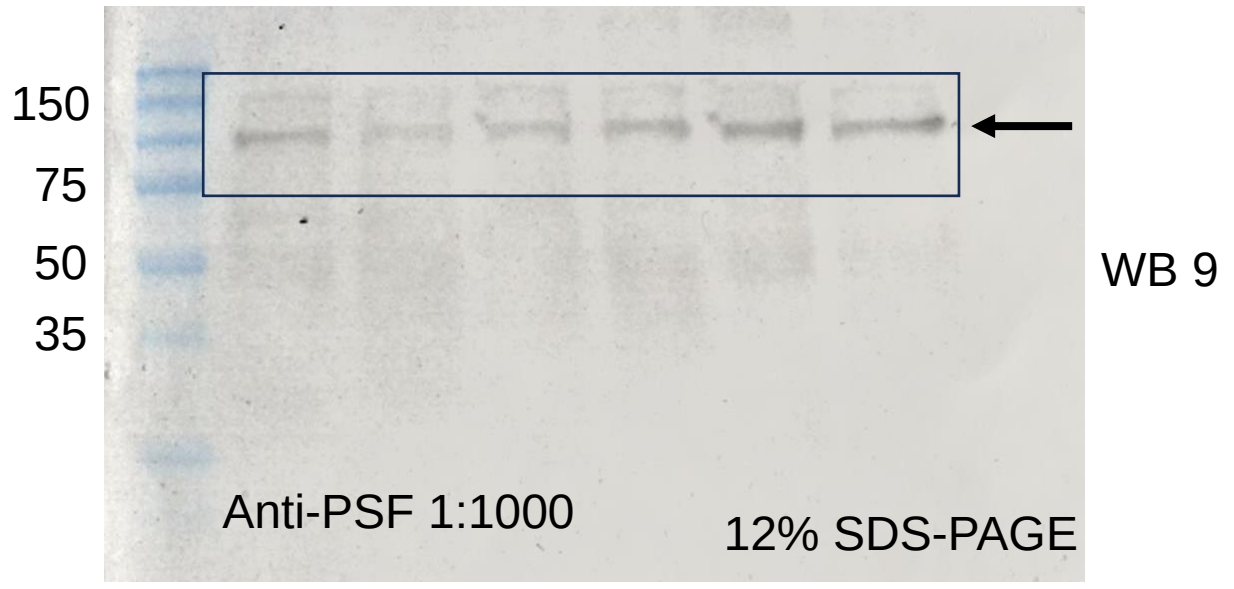

30 μg of protein each well

WB 8 and 9

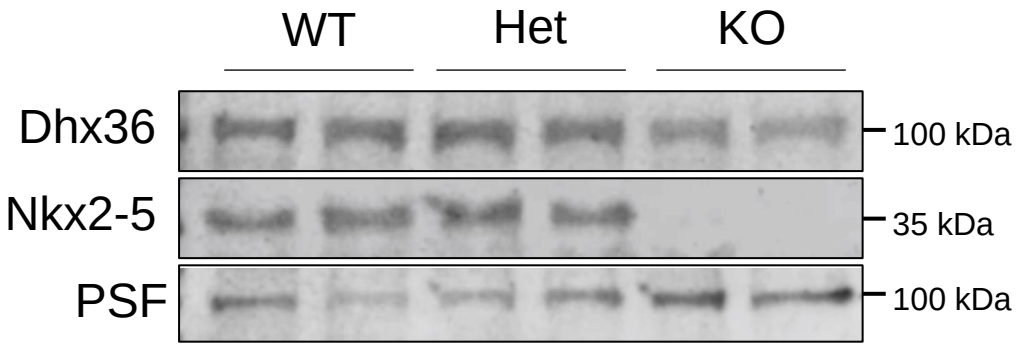

Supplementary Fig. 8a. Western blotting analysis showing reduced expression of Dhx36 and complete absence of Nkx2-5 in mutant PD7 hearts (KO; n=2), compared to heterozygous (Het; n=2) or WT (n=2). PSF (PTB-associated splicing factor) was used as a loading control in the same blot where Nkx2-5 was detected. The areas shown in Supplementary Fig. 8a are outlined in the uncropped blots of the previous page.